# Supporting Information

## Bergman et al. 10.1073/pnas.1412189111

### SI Materials and Methods

**Animals.** The morphological experiments were performed on male Wistar rats (body weight = 280–320 g) and male C57BL/6 mice (25–30 g; Scanbur BK). In addition, two glutamic acid decarboxylase 67 (GAD67) -EGFP GAD-GFP (α-neo) knockin mice (1) and two choline-acetyltransferase (ChAT) -(BAC)-EGFP mice (2) were used. The animals were maintained under standard conditions on a 12-h day/night cycle (lights on 0700 h), with water and food available ad libitum. All procedures practiced on animals were approved by the local ethical committee (Stockholms norra djurförsöksetiska nämnd) and in accordance with the policy of the Society for Neuroscience on the use of animals in neuroscience research. For physiological (EEG) experiments, male Wistar rats (Semmelweis University; weighing 300–350 g at implantation) were used. Rats were kept in single cages with food and water available ad libitum, maintained in a 12-h light/dark cycle (daylight-type fluorescent tubes, 18 W, ∼300 lx) at room temperature (RT; 21 °C ± 1 °C). Experiments were performed according to the European Communities Council Directive of November 24, 1986 (86/609/EEC) and the National Institutes of Health's Principles of Laboratory Animal Care as well as specific national laws (the Hungarian Governmental Regulations on animal studies, December 31, 1998). All experiments were approved by the National Scientific Ethical Committee on Animal Experimentation and permitted by the government (Food Chain Safety and Animal Health Directorate of the Central Agricultural Office, Permit no. 22.1/1375/7/2010). All surgery was performed under anesthesia, and all efforts were made to minimize suffering.

**Colchichine Treatment in Rats and Mice.** Altogether, 2 C57BL/6 mice and 18 Wistar rats received intracerebroventricular (icv.) injections of the mitosis inhibitor (and axoplasmic transport blocker) colchicine under Hypnorm/Midazolam anesthesia (contains Midazolam at 12.5 mg/kg, fentanyl citrate at 0.78 mg/kg, and fluanisone at 25 mg/kg i.p. and Midazolam at 6.25 mg/kg, fentanyl citrate at 0.4 mg/kg, and fluanisone at 12.5 mg/kg i.p for mice and rats, respectively). Colchicine was dissolved in 0.9% NaCl to a final concentration of 30 μg in 5 μL and 100 μg in 10 μL for mice and rats, respectively. The drug was slowly infused into the left ventricle using a Hamilton syringe with a 26-gauge needle attached. Injection coordinates were anteroposterior (AP) = 0.4 mm from bregma, lateral (L) = 1.0 mm from midline, and ventral (V) = 2.5 mm deep from the surface, and AP = 1.0 mm from bregma, L = 1.6 mm from midline, and V = 4.5 mm deep from the surface of the brain according to published atlases for mouse and rat (3, 4), respectively. The syringe was left in the brain for 5 min after injection to prevent backflow of the colchicine. Twenty-four hours later, animals were perfused and processed for immunohistochemistry.

**Fixation and Cutting.** Colchichine-treated and control (nontreated) rats (18 colchichine and 10 control) and mice (2 colchichine and 2 control) were deeply anesthetized using sodium pentobarbital (60 mg/kg i.p.; Apoteket). They were perfused through the ascending aorta with 20 or 60 mL Tyrode's buffer (37 °C) followed by 20 or 60 mL mixture of 4% (wt/wt) paraformaldehyde and 0.2% picric acid diluted in 0.16 M phosphate buffer (pH 6.9) and 50 or 300 mL of the same fixative at 4 °C in all cases for mouse and rats, respectively. The brains were dissected out, postfixed in the same fixative for 120 min at 4 °C, and finally, immersed in 10% sucrose diluted in PBS (pH 7.4) containing 0.01% sodium azide (Sigma-Aldrich) and 0.02% Bacitracin (Sigma-Aldrich) at 4 °C for 48 h. The brains were snap-frozen with $CO_2$, and pairs of colchichine-treated and control brain were sectioned at 20 μm in a cryostat (Microm) at the level of hypothalamus (starting at the decussation of anterior commissure and finishing after the supramamillary nucleus). In addition, two pairs of brains were cut at multiple levels from the bulbus olfactorius to the spinal cord. The sections were then mounted on SuperFrost Plus slides (VWR International).

**Serum/Cerebrospinal Fluid Immunostaining, Protease/Glycosidase Pretreatments, and Fluorescent Microscopy.** For serum or cerebrospinal fluid (CSF) immunostaining, sections were washed in PBS and incubated overnight at 4 °C with sera or CSF samples from individual patients or controls at a dilution of 1:1,000 or 1:25–1:100, respectively, in 0.01 M PBS containing 0.3% TritonX-100, 0.02% bacitracin, and 0.01% sodium azide. To visualize the immunoreactivity, the sections were processed using a commercial kit (PerkinElmer Life Science) based on tyramide signal amplification (5). Briefly, the sections were washed in buffer of 0.1 M Tris·HCl, pH 7.5, 0.15 M NaCl, and 0.05% Tween 20 for 15 min, incubated with buffer of 0.1 M Tris·HCl, pH 7.5, 0.15 M NaCl, and 0.5% Dupont Blocking Reagent (PerkinElmer) for 30 min at RT, and incubated with a donkey anti-human IgG coupled to HRP (Jackson Immunoresearch Europe) diluted 1:200 in 0.1 M Tris·HCl, pH 7.5, 0.15 M NaCl, and 0.5% Dupont Blocking Reagent (PerkinElmer) for 30 min. The sections were washed in buffer of 0.1 M Tris·HCl, pH 7.5, 0.15 M NaCl, and 0.05% Tween 20 and incubated in a biotinyl tyramide-FITC conjugate (PerkinElmer) diluted 1:100 in amplification diluent for 10 min at RT. Regarding the CSF immunostainings, a rabbit anti-human IgG (DAKO) was applied at the dilution of 1:600 followed by a swine anti-rabbit IgG coupled to HRP (1:200; DAKO) and tyramide signal amplification$^+$ visualization. In case of GAD67-EGFP and ChAT-EGFP sections, the serum immunostaining was developed with tetramethylrhodamine (PerkinElmer) diluted 1:500 in amplification diluent for 10 min at RT.

For glycosidase pretreatment, sections were preincubated in 250 mM sodium phosphate buffer (pH 7.2) and incubated in a glycosidase enzyme mixture containing peptide-*N*-glucosidase, sialidase, β-gal, glucosaminidase, and O-glycosidse to remove all N-linked oligosaccharides and most O-linked sugars from glycoproteids (Enzymatic DeGlycoMX Kit, KE-DGMX, lot no. 912.1C; QA Bio) in the same buffer for 6 or 24 h at 37 °C in a humid chamber. Six-hour glycosidase incubation completely abolished Gl7 immunoreactivity in adjacent brain sections (positive control; Gl7 is a sialic acid epitope found recently also in the brain) (6). In case of protease treatment, sections were preincubated in Tris·EDTA buffer (pH 8.0) and then incubated with 1 or 2 μg/mL proteinase K (Quagen) in the same buffer for 20 min at 37 °C in a humid chamber. In case of both protease and glycosidase treatments, control sections were incubated together with the digested sections in buffers without enzymes at 37 °C.

After the immunoreactions, sections were coverslipped using 2.5% 1.4-diazabicyclo[2.2.2.]octane (DABCO) in glycerol (Sigma). The sections were examined using a Nikon Eclipse E600 fluorescence microscope with objective lenses 4×, 10×, and 20× (Nikon) equipped with appropriate filters and an ORCA-ER C4742-80 digital camera (Hamamatsu Photonics K.K., System Division) using Hamamatsu Photonics Wasabi 150 software.

**Double Labeling and Confocal Analysis.** For double labeling, serum-immunostained sections were washed in 0.01 M PBS extensively and incubated for one or two nights at 4 °C with primary antibodies in 0.01 M PBS (Table S2). After washing in 0.01 M PBS, the sections were incubated with Cy3-conjugated anti-rabbit IgG, Cy3-conjugated anti-mouse IgG, or rhodamine-conjugated anti-sheep IgG secondary antibodies (Jackson Immunoresearch Europe) at a dilution of 1:150 (Cy3) or 1:80 (rhodamine) in 0.01 M PBS for 90 min. After the immunoreactions, sections were coverslipped using 2.5% DABCO in glycerol (Sigma) and examined with a Zeiss LSM 510 Meta confocal system installed on a Zeiss Axioplan 2 microscope equipped with 10× (N.A. of 0.45), 20× (N.A. of 0.75), and 100× (N.A. of 1.40) oil objectives. The FITC labeling and EGFP fluorescence (GAD67-EGFP and ChAT-EGFP) were excited using the 488-nm argon laser, and its signal was detected using the HQ 530/60 emission filter. For the detection of tetramethylrhodamine, rhodamine, and Cy3, the 543-nm HeNe laser combined with HQ 590/70 emission was used. Digital images from the microscopy were slightly modified to optimize for brightness, and contrast using ZEN 2011 (Carl Zeiss Microimaging Gmbh) and Adobe Photoshop 7.0 software (Adobe Systems) to best represent the immunohistochemistry observed at the microscope.

For the quantitative evaluation of the number of melanin-concentrating hormone (MCH)/serum- or proopiomelanocortin (POMC)/serum-immunoreactive cells, 7–7 MCH/serum and POMC/serum double-stained sections were selected from different rostrocaudal levels of the hypothalamus. In case of the MCH/serum sections, three optically layered and merged micrographs were taken from each section: one from zona incerta/subzona incerta, one from the perifornical part of lateral hypothalamus, and one from the peduncular part of the lateral hypothalamus. Each micrograph included four or five 3-μm-thick optical layers (20× objective and 1.5× optical zoom). The number of $MCH^+/serum^-$, $MCH^-/serum^+$, and $MCH^+/serum^+$ neurons was determined in each micrograph on the screen by the same observer. Similarly, two optically layered and merged micrographs were taken in each section bilaterally from the arcuate nucleus, and the number of $POMC^+/serum^-$, $POMC^-/serum^+$, and $POMC^+/serum^+$ neurons was determined as above.

**Absorption Experiments in Dot Blot and Immunohistochemistry.** For dot blots, the sample (1 μL) was spotted onto a nitrocellulose membrane (Amersham Biosciences), left to dry, and fixed with 0.05% glutaraldehyde in PBS for 30 min. The membrane was then washed with PBS three times for 10 min, blocked for 1 h in PBS containing 5% (wt/vol) fat-free milk, and incubated overnight with serum diluted 1:5,000. The second antibody was an anti-human IgG conjugated with HRP (Jackson) diluted 1:50,000. To visualize the results, an ECL Western blot detection system was used (GE Healthcare).

For immunohistochemical absorption control experiments, prediluted sera (1:1,000) were incubated overnight at 4 °C with $10^{-6}$–$10^{-3}$ M peptides, and these mixtures were applied as primary antibodies in the subsequent immunostainings.

**Preparation of IgG from Patients' Sera.** Purified IgG antibodies were prepared from two narcoleptic sera: one of them without immunostaining pattern [nonpattern (NP); NP-IgG] and one of them with the neuropeptide glutamic acid-isoleucine/α–melanocyte-stimulating hormone (NEI/αMSH) pattern (NEI/αMSH-IgG). Both individuals were Pandemrix-related narcoleptic [(*i*) age of onset: 16 y, date of onset: December of 2009, sample collection for IgG purification: March of 2012; (*ii*) age of onset: 17 y, date of onset: January of 2010, sample collection for IgG purification: March of 2012]. In addition, an IgG preparation from a Pandemrix-vaccinated healthy control (HC) individual was also prepared (HC-IgG; age at sample collection: 37 y, sample collection: October of 2012).

For the purification, we used HiTrap Protein G 1-mL affinity columns packed with protein G Sepharose High Performance (GE Healthcare) according to the producer's instructions. Briefly, aggregates in the sera were discarded by centrifugation for 10 min at 10,000 × *g*. The pH and ionic strength of the supernatants were adjusted by dilution (10 times) with the binding buffer 20 mM Na-phosphate (pH 7.0). The columns were first equilibrated with binding buffer, and then, the diluted sera were applied followed by subsequent washing with binding buffer. Finally, the IgG antibodies were eluted with 0.1 M glycine·HCl (pH 2.7) and collected in tubes containing 60 μL 1 M Tris·HCl (pH 9) to preserve the function of acid-sensitive antibodies. For desalting of IgG fractions, PD-10 columns packed with Sephadex G-25M (GE Healthcare) were used. The PD-10 columns were first equilibrated with milliQ water followed by application of 2.5 mL IgG fraction and then eluted with 3.5 mL milliQ water. Finally, these eluates were lyophilized and redissolved in artificial CSF (TOCRIS). The final concentration of IgG preparations was adjusted to 65 mg/mL, and 13-μL aliquots were stored at −80 °C until the physiological experiments. Purified NEI/αMSH-IgG preparation exhibited the same NEI/αMSH immunostaining pattern as the initial serum itself (at 1:10,000 or 1:5,000 dilutions).

**Physiological Experiments 1: Intracerebroventricular Injection of Purified IgGs, EEG Registration, and Evaluation of Sleep Time Data.** Animals were equipped with electroencephalogram (EEG) and electromyogram (EMG) electrodes as described earlier (7, 8). At the same time, an icv. cannula was stereotaxically implanted into the right lateral ventricle (8). On the day of the experiment, at the beginning of inactive phase (at light onset), IgG preparations (65 mg/mL) were administered for each animal under halothane anesthesia [2% (vol/vol)] in a volume of 10 μL through a glass Hamilton syringe connected to a polythene tube and an injection cannula. The injection cannula was kept in place for an extra 1 min before removal. After injection, rats woke up in 1–2 min and were reattached to the flexible recording cable; 24-h video, EEG, EMG, and motility were recorded for each animal before the icv. injections [baseline (BL)] and during days 2 and 15 after the injections. Food intake and body weight were monitored during the entire experiment.

The vigilance states were classified by SleepSign for Animal sleep analysis software (Kissei Comtec America, Inc.) for 4-s periods using conventional criteria followed by visual supervision. The vigilance stages were differentiated as described earlier (7, 8). In the sleep analysis of the BL and days 2 and 15, the following vigilance parameters were calculated: time spent in wake and rapid eye movement sleep (REM) as well as light slow-wave sleep (SWS1) and deep SWS (SWS2) per hour. Sleep fragmentation was defined as the number of awakenings after a sleep stage (SWS1, SWS2, REM, and intermediate stage of sleep). An REM episode was defined as an REM item lasting at least 16 s and not interrupted more than 16 s by other stages (9). Sleep-onset REM was calculated as an REM (SOREMP) episode in the inactive or active phase that occurred after ≥2 min of wake with <2 min of an intervening episode of SWS (10). Most statistical analyses on sleep time data were carried out by two-way repeated measure ANOVA matched by pairs (repeated factor: from 1 to 6 h). For posthoc analysis (for every 1 h from 1 to 6 h), Bonferroni multiple comparisons test was used. One-way repeated measure ANOVA and Tukey posthoc test were applied with the statistical evaluation of the number of transitions from non-REM (NREM) to wake and from NREM to REM stages as well as the number of REM sleep episodes. Each group was compared with its own BL. All statistical analyses and Fig. 6 *A*–*O* were prepared by the GraphPad Prism 6.03 demo program.

**Physiological Experiments 2: Examination of the Spectral Distribution of EEG Power.** Adopting the state space technique after the work by Diniz Behn et al. (11), we plotted ratio 1 (6.5–9/0.25–9 Hz)

on the abscissa and ratio 2 (0.25–20/0.25–60 Hz) on the ordinate defining 2D spectra for any of the sera-treated groups (HC-IgG, NP-IgG, and NEI/αMSH-IgG) to separate clusters corresponding to the conventionally determined sleep stages, like REM, NREM, and wake. Ratio 1 was determined to emphasize high θ-activity (6.5–9 Hz) (11), which dominates REM in rodents. Alteration of this frequency range can be crucial, because dysregulation of REM is typical in narcolepsy. Although this range is slightly different from that applied generally as the θ-range in rat (5–9 Hz), we used the 6.5- to 9-Hz range, because cluster separation was more efficient using this range. Ratio 2 (0.3–20/0.3–55 Hz) was developed to separate NREM and wake (11). We adopted this range with little modification (0.25–20/0.25–60 Hz), because our setup measures the frequency range of 0.25–60 Hz. On the spectra, each point represented EEG power data of a 4-s epoch of the 6-h-long EEG recordings (of each animal of the groups) in active and inactive phases of recordings. Then, (*i*) to avoid that the several tens of thousands data points covering up each other (losing the quantitative information) and (*ii*) to visualize not only dispersion but also, density of power data of clusters, we made heat map spectra using a JavaScript-based visualization script. Using this color-coded density map, we were able to depict the quantity of data points of a certain coordinate, which with the built-in blurring function of the heat map script, led to the representation of the three different clusters corresponding to wake, NREM, and REM sleep stages. To visualize the general position of state space clusters associated with REM, NREM, and wake stages, we depicted BL recordings in Fig. 7. These state space clusters, corresponding to the REM, NREM, and wake stages, seemed to be conserved in the BL recordings. Although the heat maps represent the BL datasets, where the stage cluster centriods are indicated by black dots in Fig. 7, we also plotted the stage cluster centriods of day 2 by white dots in Fig. 7 to show the direction and the degree of the shifts. Centroids were calculated by averaging EEG power data (arithmetic mean calculated from the $x$ and $y$ coordinates of each epoch) of animals within groups in active and inactive phase on BL and day 2. Distances between centroids were evaluated by paired $t$ tests (day 2 vs. BL).


1. Tamamaki N, et al. (2003) Green fluorescent protein expression and colocalization with calretinin, parvalbumin, and somatostatin in the GAD67-GFP knock-in mouse. *J Comp Neurol* 467(1):60–79.
2. Tallini YN, et al. (2006) BAC transgenic mice express enhanced green fluorescent protein in central and peripheral cholinergic neurons. *Physiol Genomics* 27(3): 391–397.
3. Paxinos G, Franklin KBJ (2007) *The Mouse Brain in Streotaxic Coordinates* (Elsevier, Amsterdam), 3rd Ed.
4. Paxinos G, Watson C (2007) *The Rat Brain in Stereotaxic Coordinates* (Elsevier, Amsterdam), 6th Ed.
5. Adams JC (1992) Biotin amplification of biotin and horseradish peroxidase signals in histochemical stains. *J Histochem Cytochem* 40(10):1457–1463.
6. Deckert-Schlüter M, Buck C, Schlüter D (1999) Kinetics and differential expression of heat-stable antigen and GL7 in the normal and Toxoplasma gondii-infected murine brain. *Acta Neuropathol* 98(1):97–106.
7. Kantor S, Jakus R, Balogh B, Benko A, Bagdy G (2004) Increased wakefulness, motor activity and decreased theta activity after blockade of the 5-HT2B receptor by the subtype-selective antagonist SB-215505. *Br J Pharmacol* 142(8):1332–1342.
8. Vas S, et al. (2013) Nesfatin-1/NUCB2 as a potential new element of sleep regulation in rats. *PLoS ONE* 8(4):e59809.
9. Kitka T, et al. (2009) Small platform sleep deprivation selectively increases the average duration of rapid eye movement sleep episodes during sleep rebound. *Behav Brain Res* 205(2):482–487.
10. Gerashchenko D, et al. (2001) Hypocretin-2-saporin lesions of the lateral hypothalamus produce narcoleptic-like sleep behavior in the rat. *J Neurosci* 21(18):7273–7283.
11. Diniz Behn CG, Klerman EB, Mochizuki T, Lin SC, Scammell TE (2010) Abnormal sleep/wake dynamics in orexin knockout mice. *Sleep* 33(3):297–306.

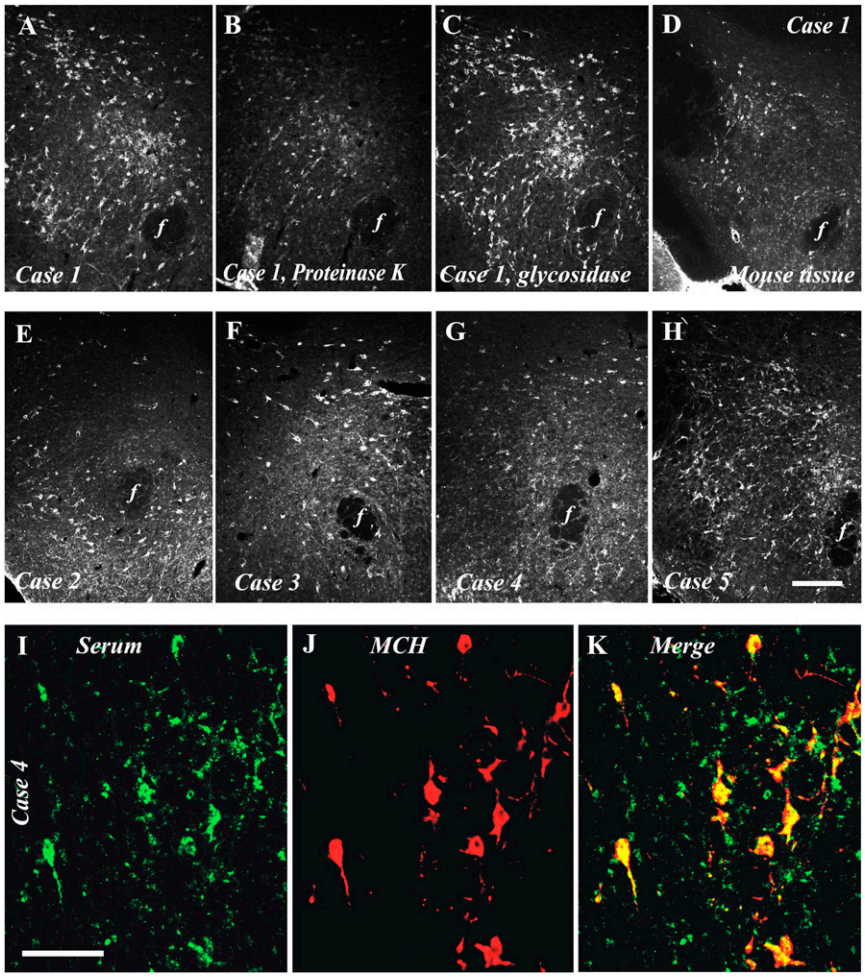


**Fig. S1.** (*A* and *B*) The NEI/αMSH immunostaining pattern (pattern A) is strongly reduced after a 20-min 1-μg/mL proteinase K predigestion (*B* vs. *A*; digested vs. shame-digested control). (*C*) In contrast, the immunostaining intensity is even higher after a 6-h glycosidase pretreatment. (*D*) This pattern can also be detected in sections from colchichine-treated mouse hypothalamus. (*E–H*) Immunostaining in the perifornical area of colchichine-treated rat showing four additional NEI/αMSH pattern narcoleptic sera (the micrographs are from slightly different coronal levels). (*A* and *E–H*) All five pattern A sera (cases 1–5) selectively stained the MCH and POMC neuronal populations in the hypothalamus, albeit with different intensities. (*I* and *K*) Only cases verified with double labeling (serum + MCH/β-endorphin antiserum) were listed as pattern A sera (e.g., case 4). *f*, fornix. (Scale bars: *A–H*, 200 μm; *I–K*, 50 μm.)

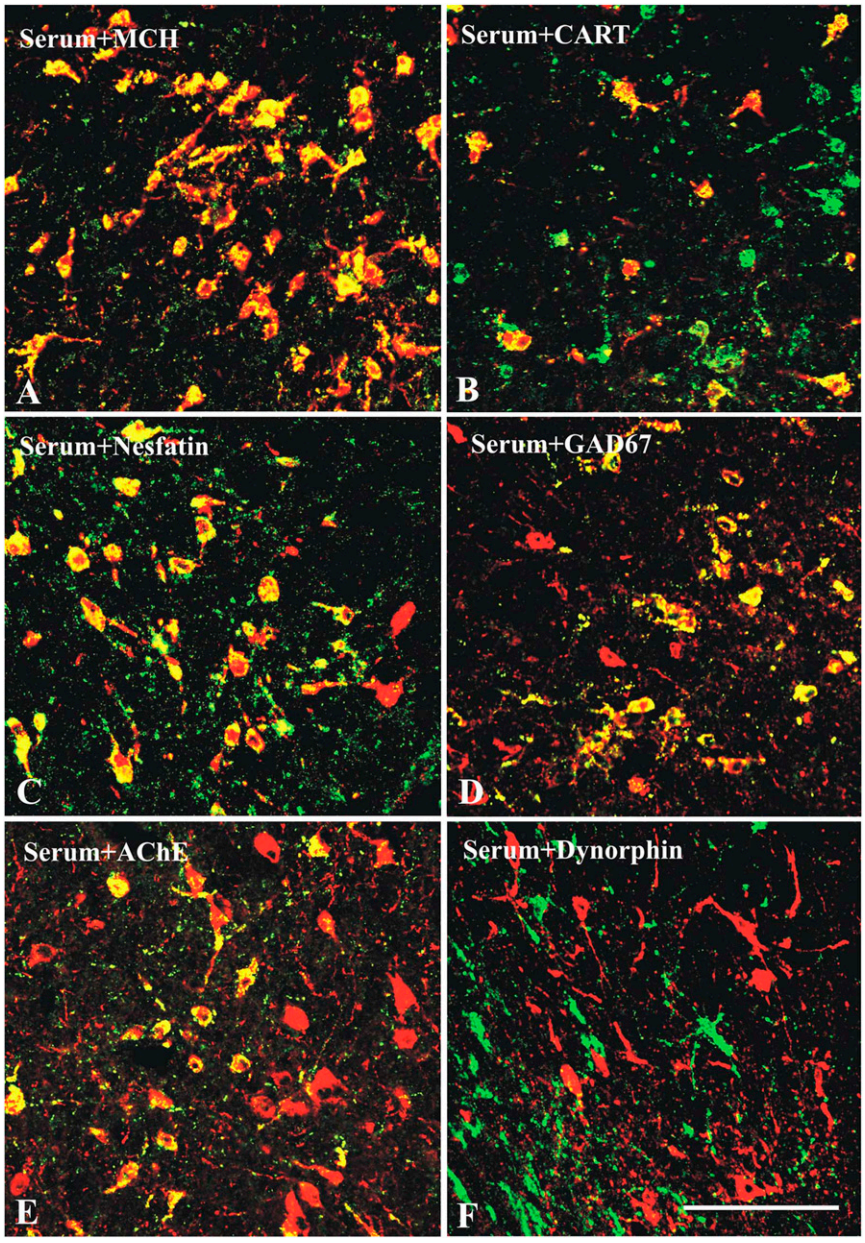


**Fig. S2.** Additional neurochemical characterization of the NEI/αMSH immunostaining pattern in the zona incerta-lateral hypothalamus (colchicine-treated rat). (*A*) Serum-positive cells are always immunoreactive for MCH, and (*B*) many of them are also immunoreactive for cocaine- and amphetamine-regulated transcript (CART). Most of the (*C*) nesfatin-immunoreactive and many of the (*D*) GAD67-immunoreactive and (*E*) acetylcholine esterase (AChE) -immunoreactive neurons are also serum-positive in this region. (*F*) However, no cells are double labeled for serum/dynorphin. Green channel, serum immunostaining; red channel, immunostaining for MCH, CART, GAD67, AChE, and dynorphin. (Scale bar: 100 μm.)

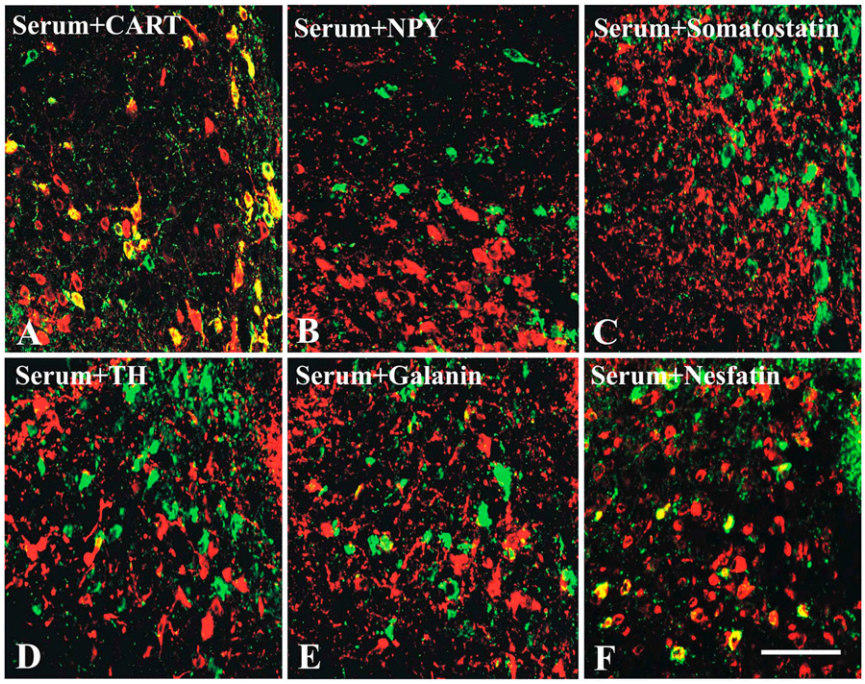


**Fig. S3.** Additional neurochemical characterization of the NEI/αMSH immunostaining pattern in the arcuate nucleus (colchicine-treated rat). Serum-positive arcuate neurons are often immunoreactive for (*A*) cocaine- and amphetamine-regulated transcript (CART) but never for (*B*) neuropeptide tyrosine (NPY), (*C*) somatostatin, (*D*) tyrosine hydroxylase (TH), or (*E*) galanin. (*F*) Many nesfatin-immunoreactive arcuate cells are serum-positive. Green channel, serum immunostaining; red channel, immunostaining for CART, NPY, somatostatin, TH, galanin, and nesfatin. (Scale bar: 100 μm.)

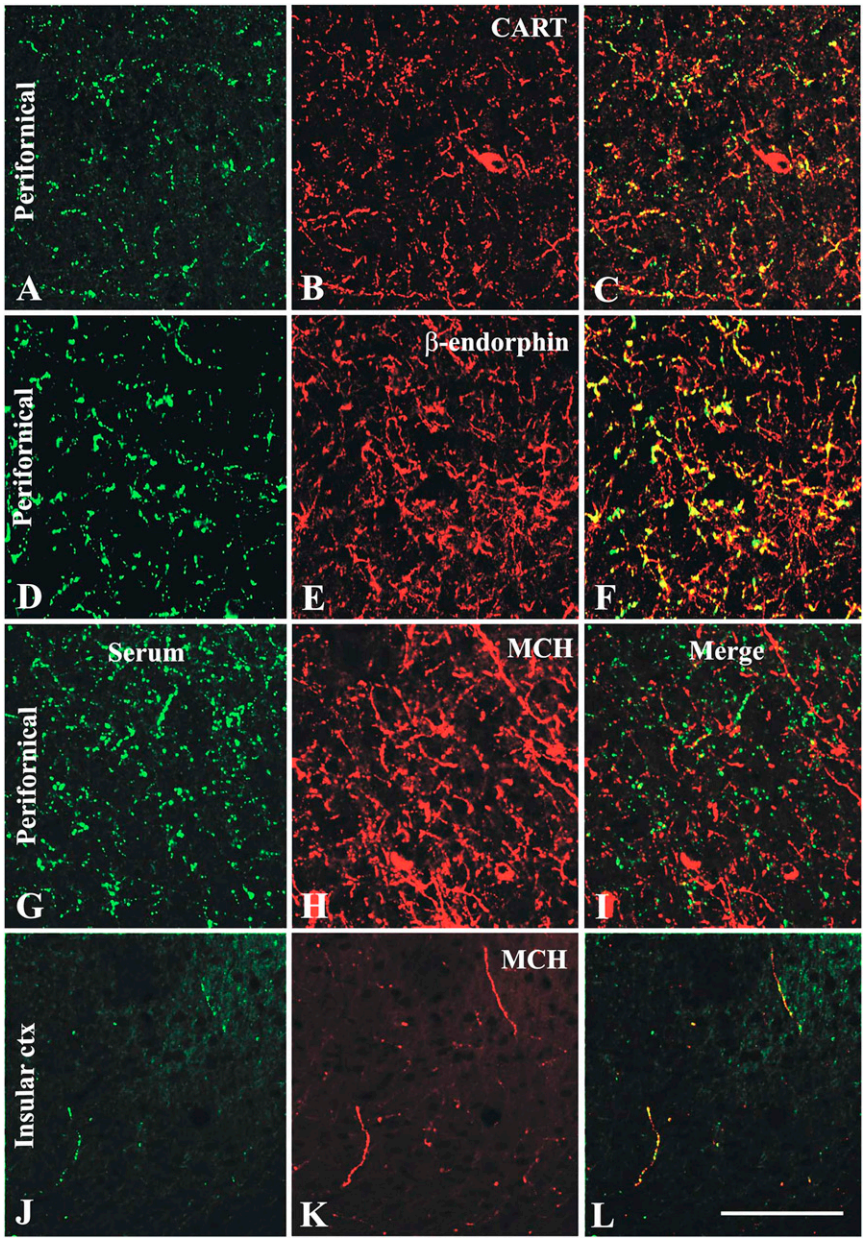


**Fig. S4.** The dense serum-positive fiber network in the perifornical lateral hypothalamus highly colocalizes (*A–C*) cocaine- and amphetamine-regulated transcript (CART) and (*D–F*) β-endorphin but not (*G–I*) MCH. (*J–L*) Sparse cortical fibers are double stained for serum and MCH. All micrographs from sections of a control rat (no colchichine) immunostained with a narcoleptic NEI/αMSH pattern serum plus peptide antiserum. ctx, cortex. (Scale bar: 100 μm.)

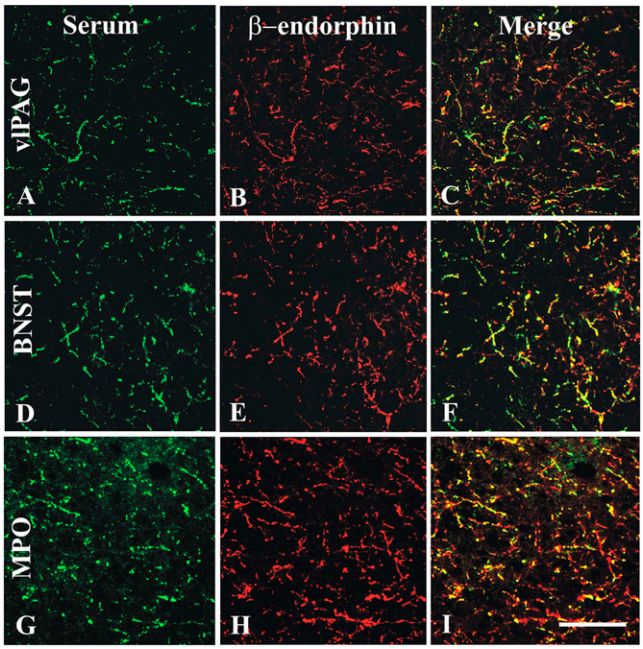


**Fig. S5.** The dense serum-positive fiber network in (*A–C*) the ventrolateral periaqueductal gray (vlPAG), (*D–F*) the bed nucleus of stria terminalis (BNST), or (*G–I*) the medial preoptic area (MPA) highly colocalizes β-endorphin. All micrographs from sections of a control rat (no colchichine) immunostained with a narcoleptic NEI/αMSH pattern serum plus peptide antiserum. (Scale bar: 100 μm.)

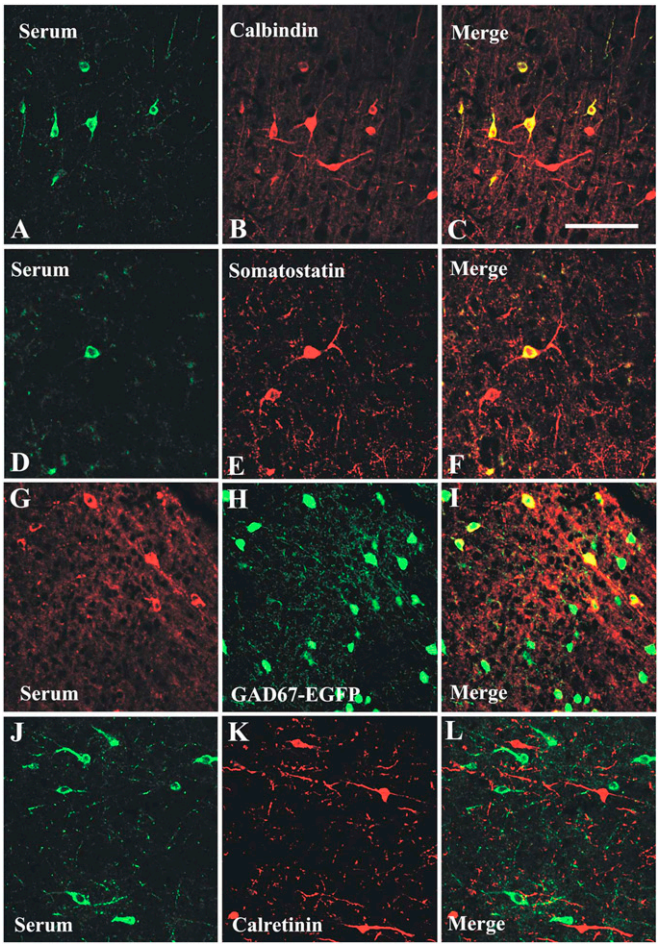


**Fig. S6.** Characterization of the cortical interneuron pattern (pattern B). (*A–C*) In most group B cases, serum-immunoreactive neurons are calbindin-immunoreactive. (*D–F*) Some serum-positive neurons are also immunoreactive for somatostatin. (*G–I*) All serum-immunoreactive neurons express GAD67-EGFP, but (*J–L*) in almost all cases, they do not express calretinin. The micrographs were taken from the parietal cortex of colchicine-treated rat. (Scale bar: 150 μm.)

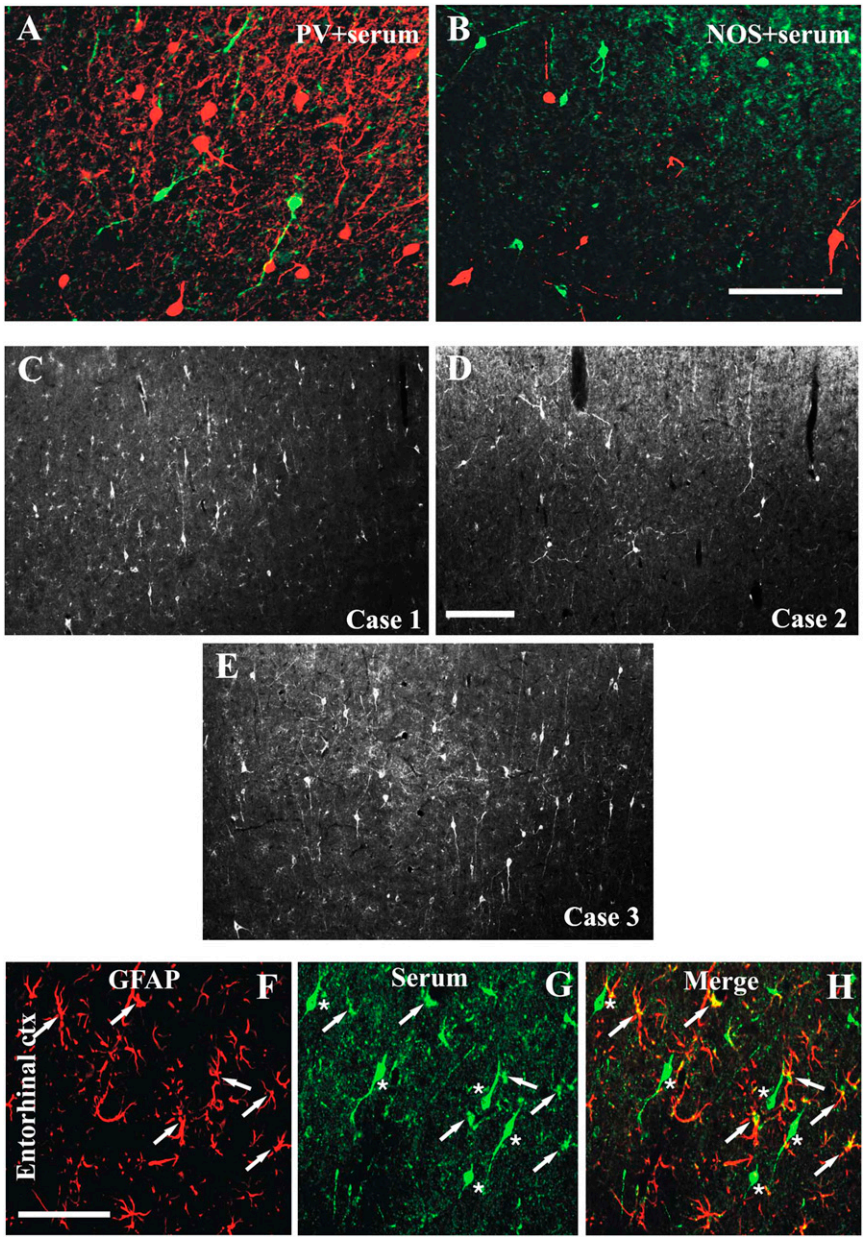


**Fig. S7.** Additional neurochemical characterization of the cortical interneuron pattern (pattern B). No serum-positive cells are immunoreactive for (*A*) parvalbumin (PV) or (*B*) NOS in any of the group B cases. (*C–E*) Three examples (cases 1–3) of immunostaining with pattern B sera in the parietal cortex. (*F–H*) Especially in entorhinal-piriform cortices, pattern B sera also stained cells positive for GFAP (that is, astrocytes). *Serum-positive interneurons. Arrows point to double-stained astroglial cells. Green channel, serum immunostaining; red channel, PV, NOS, and GFAP. ctx, cortex. (Scale bars: *A* and *B*, 200 μm; *C–E*, 200 μm; *F–H*, 100 μm.)

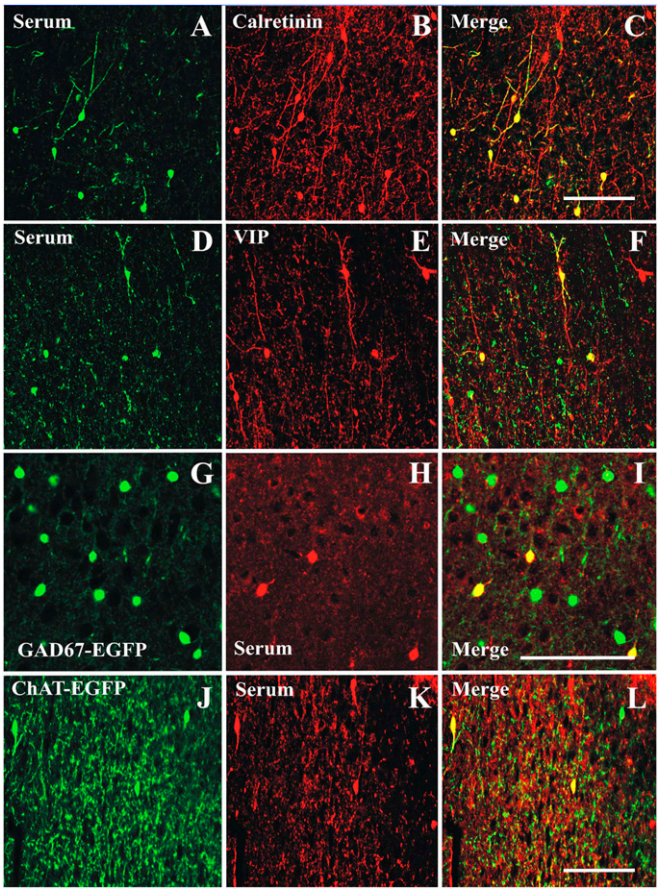


**Fig. S8.** (*A–C*) In one exceptional group B case, most but not all serum-immunoreactive neurons are calretinin-immunoreactive. In this particular case, some serum-positive neurons are also immunoreactive for (*D–F*) vasoactive intestinal polypeptide (VIP) and (*J–L*) ChAT-EGFP, and (*G–I*) all serum-immunoreactive neurons express GAD67-EGFP. The micrographs were taken from insular cortex. (Scale bar: 150 μm.)

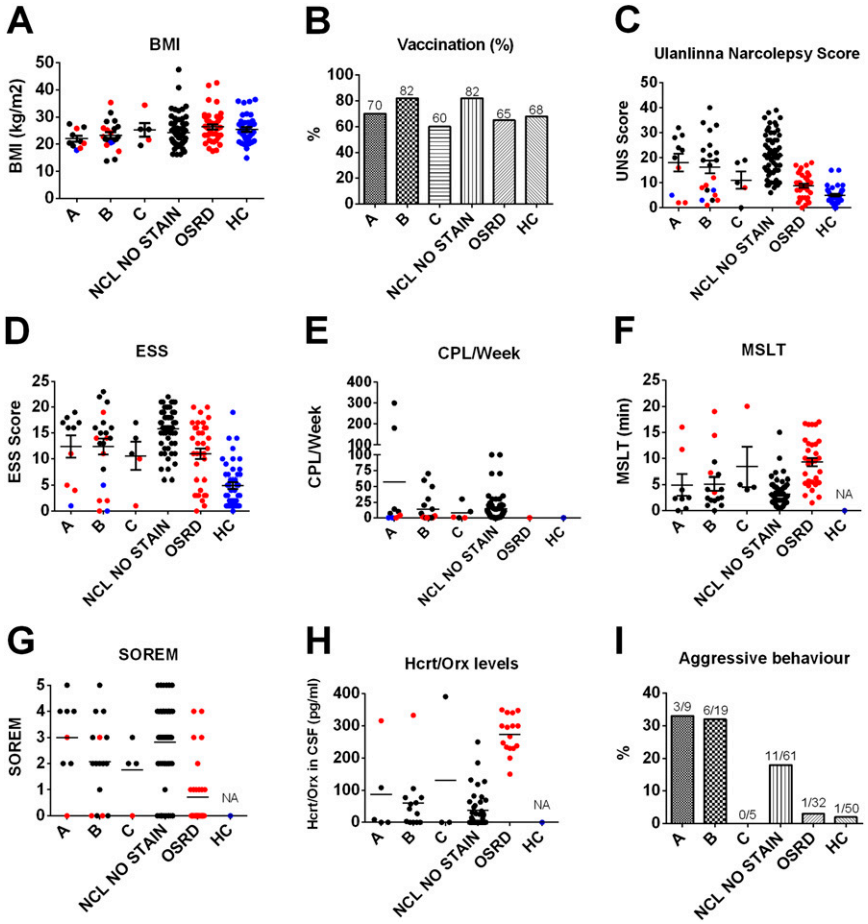


**Fig. S9.** (*A–I*) Relation between staining patterns and clinical parameters. Narcolepsy patients with staining patterns A, B, and C were compared with narcolepsy patients without these patterns (no stain [NCL]) and patients with other sleep-related disorders (OSRDs; red dots) and healthy controls from the Helsinki Sleep Clinic/VitalMed Research Centre (HC; blue dots). Black dots represent narcolepsy patients. Notably, some OSRD patients as well as some HCs exhibited staining pattern A, B, or C (marked with red and blue dots, respectively). BMI, body mass index; CPL, cataplexy; CTRL, control; ESS, Epworth Narcolepsy Score; MSLT, multiple sleep latency test; Hcrt/Orx, hypocretin/orexin; SOREM, sleep-onset REM sleep; UNS, Ullanlinna Narcolepsy Score.

**Table S1. Data for patients and controls in the study**

| | Narcolepsy | OSRD | Helsinki Sleep Clinic controls | Military controls |
|---|---|---|---|---|
| Total number of patients (*n*) | 92 | 55 | 85 | 60 |
| No sera available (*n*) | 3 | 3 | 8 | 0 |
| Patients included in analysis (*n*) | 89 | 52 | 77 | 60 |
| Male (*n*) | 34 (38%) | 17 (33%) | 31 (40%) | 60 (100%) |
| Female (*n*) | 56 (62%) | 35 (67%) | 47 (60%) | 0 |
| Age (y) at sample median (range) | 19 (8–65) | 29 (14–71) | 45 (6–70) | Young men |
| Age (y) at onset median (range) | 15 (2–62) | NA | NA | NA |
| Age (y) at onset vaccinated median (range) | 15 (6–62) | NA | NA | NA |
| Age (y) at onset nonvaccinated median (range) | 15 (2–42) | NA | NA | NA |
| Influenza-like illness (*n*) | 3/75 (4%) | 2/30 (6.7%) | 1/22 (4.5%) | ND |
| H1N1 vaccination (*n*) | 72/88 (82%) | 28/43 (65%) | 32/47 (68%) | 10/60 (17%) |
| Pandemrix-related (*n*) | 53/86 (62%) | NA | NA | NA |
| BMI mean (kg/m$^2$) | 24.0 | 25.9 | 25.1 | ND |
| UNS mean | 21.7 | 8.0 | 5.0 | ND |
| UNS ≥ 14 | 67/81 (83%) | 8/46 (17%) | 2/41 (5%) | |
| ESS mean | 15.9 | 10.2 | 4.8 | ND |
| ESS ≥ 11 | 73/81 (90%) | 28/47 (60%) | 4/48 (8%) | |
| CPL/wk mean (range) | 20.5 (0–300) | 0 (0–1) | 0 | 0 |
| Orexin in CSF mean (range) | 41.9 (0–391)* | 279.0 (150–350) | NA | NA |
| Orexin < 110 pg/mL (*n*) | 50/57 (88%) | 0/18 (0%) | NA | NA |
| MSLT median (range) | 3.1 (0–15)[†] | 10.0 (1.5–20) | NA | NA |
| SOREMPS median (range) | 3 (0–5) | 0 (0–4)[‡] | NA | NA |
| Suspected RBD (*n*) | 56/76 (74%) | 16/45 (36%) | 4/42 (10%) | ND |
| HLA DQB1*06:02-positive | 67/69 (97%) | 19/42 (45%) | 44/70 (63%) | ND |

The denominator is given when data are missing. BMI, body mass index; CPL, cataplexy; DQB1*06:02, a common HLA type among narcolepsy patients; ESS, Epworth Sleep Score; MSLT, Multiple Sleep Latency Test; NA, not applicable; ND, not determined; OSRD, other sleep-related disorder; RBD, REM sleep behavior disorder; SOREMPS, sleep-onset REM periods; suspected RBD, possible RBD based on the Marburg RBD screening questionnaire; UNS, Ullanlinna Narcolepsy Score.

*The subject with Hcrt 391 pg/mL had positive MSLT for narcolepsy, hypnagogic hallucinations, and sleep paralyses.

[†]Three subjects with narcolepsy had mean sleep latency > 8 min. They were all HLA 06:02-positive, had unambiguous cataplexy, and were hypocretin/orexin-deficient.

[‡]One patient with Kleine–Levin syndrome had four SOREMPs, and one patient with bipolar disorder had three SOREMPs.

**Table S2. List and specification of antibodies used for double labeling with human sera**

| Primary antibody | Type of antibody | Dilution for normal fluorescence IHC | Dilution for TSA IHC (absorption controls) | Source | Catalog no./ref. |
|---|---|---|---|---|---|
| MCH | Rabbit polyclonal | 1:800 | 1:8,000 | Phoenix Pharmaceuticals | H-070–47 |
| Hypocretin/orexin | Rabbit polyclonal | 1:500 | | L. de Lecea, Stanford University, Stanford, CA | de Lecea et al. (1) |
| αMSH | Rabbit polyclonal | 1:1,000 | 1:10,000 | Phoenix Pharmaceuticals | H-043–01 |
| NEI | Rabbit polyclonal | 1:1,000 | 1:10,000 | Phoenix Pharmaceuticals | H-070–49 |
| Cocaine- and amphetamine-regulated transcript | Rabbit polyclonal | 1:800 | 1:8,000 | Phoenix Pharmaceuticals | H-003–62 |
| Nesfatin | Rabbit polyclonal | 1:4,000 | | Phoenix Pharmaceuticals | H-003–22 |
| Acetylcholinesterase | Rabbit polyclonal | 1:400 | | J. Massoulié, Ecole Supérieur, Paris | Marsh et al. (2) |
| Dynorphin | Rabbit polyclonal | 1:500 | | G. Balkalkin, Uppsala University, Uppsala | Hara et al. (3) |
| β-Endorphin | Rabbit polyclonal | 1:2,000 | | Peninsula | T-4040 (RGG-8616) |
| Vasoactive intestinal polypeptide | Rabbit polyclonal | 1:400 | | ImmunoStar | 20077 |
| NOS | Sheep polyclonal | 1:600 | | P. Emson, University of Cambridge, Cambridge, UK | Herbison et al. (4) |
| Tyrosine hydroxylase | Rabbit polyclonal | 1:800 | | M. Goldstein, New York University Medical Center, New York | Markey et al. (5) |
| Somatostatin | Rabbit polyclonal | 1:800 | | R. Benoit, The Salk Institute, La Jolla, CA | Benoit et al. (6) |
| Galanin | Rabbit polyclonal | 1:800 | | E. Theodorsson, University of Linköping, Linköping, Sweden | Theodorsson and Rugarn (7) |
| Iba-1 | Rabbit polyclonal | 1:800 | | Wako | 019–19741 |
| Glial fibrillary acidic protein | Rabbit polyclonal | 1:800 | | Sigma | G2969 |
| Calbindin DK28 | Rabbit polyclonal | 1:1,500 | | Swant | CB38 |
| Parvalbumin | Rabbit polyclonal | 1:1,500 | | Swant | PV25 |
| Neuropeptide Y | Rabbit polyclonal | 1:800 | | E. Theodorsson | Theodorsson-Norheim et al. (8) |
| Calretinin | Rabbit polyclonal | 1:800 | | Swant | 7699/4 |
| GAD67 | Mouse monoclonal | 1:100 | | Millipore/Chemicon | MAB5406 |
| Syntaxin 6 (Golgi marker) | Mouse monoclonal | 1:100 | | Sigma | S9067, clone 3D10 |
| Protein-diffuse isomerase (ER marker) | Mouse monoclonal | 1:100 | | Novus Biologicals | NB300-517, clone RL90 |

IHC, immunohistochemistry; TSA, tyramide signal amplification.


1. de Lecea L, et al. (1998) The hypocretins: Hypothalamus-specific peptides with neuroexcitatory activity. *Proc Natl Acad Sci USA* 95(1):322–327.
2. Marsh D, Grassi J, Vigny M, Massoulié J (1984) An immunological study of rat acetylcholinesterase: Comparison with acetylcholinesterases from other vertebrates. *J Neurochem* 43(1): 204–213.
3. Hara Y, Yakovleva T, Bakalkin G, Pickel VM (2006) Dopamine D1 receptors have subcellular distributions conducive to interactions with prodynorphin in the rat nucleus accumbens shell. *Synapse* 60(1):1–19.
4. Herbison AE, Simonian SX, Norris PJ, Emson PC (1996) Relationship of neuronal nitric oxide synthase immunoreactivity to GnRH neurons in the ovariectomized and intact female rat. *J Neuroendocrinol* 8(1):73–82.
5. Markey KA, Kondo H, Shenkman L, Goldstein M (1980) Purification and characterization of tyrosine hydroxylase from a clonal pheochromocytoma cell line. *Mol Pharmacol* 17(1):79–85.
6. Benoit R, Böhlen P, Brazeau P, Ling N, Guillemin R (1980) Isolation and characterization of rat pancreatic somatostatin. *Endocrinology* 107(6):2127–2129.
7. Theodorsson E, Rugarn O (2000) Radioimmunoassay for rat galanin: Immunochemical and chromatographic characterization of immunoreactivity in tissue extracts. *Scand J Clin Lab Invest* 60(5):411–418.
8. Theodorsson-Norheim E, Hemsén A, Lundberg JM (1985) Radioimmunoassay for neuropeptide Y (NPY): Chromatographic characterization of immunoreactivity in plasma and tissue extracts. *Scand J Clin Lab Invest* 45(4):355–365.

**Table S3. List and specification of peptides that were applied for absorption experiments**

| Peptide | Sequence | Dilutions for absorption (M) | Source; catalog no. |
|---|---|---|---|
| Cocaine- and amphetamine-regulated transcript | pGlu - Glu - Asp - Ala - Glu - Leu - Gln - Pro - Arg - Ala - Leu - Asp - Ile - Tyr - Ser - Ala - Val - Asp - Asp - Ala - Ser - His - Glu - Lys - Glu - Leu - Ile - Glu - Ala - Leu - Gln - Glu - Val - Leu - Lys - Lys - Leu - Lys - Ser | $10^{-6}$–$10^{-4}$ | Phoenixpeptide; 003–63 |
| MCH | Asp - Phe - Asp - Met - Leu - Arg - Cys - Met - Leu - Gly - Arg - Val - Tyr - Arg - Pro - Cys - Trp - Gln - Val ~ disulfide bridge between Cys7 and Cys16 | $10^{-6}$–$10^{-4}$ | Phoenixpeptide; 070–47 |
| NEI | Glu - Ile - Gly - Asp - Glu - Glu - Asn - Ser - Ala - Lys - Phe - Pro - Ile - $NH_2$ | $10^{-6}$–$10^{-4}$ | Phoenixpeptide; 070–49 |
| αMSH | Ac - Ser - Tyr - Ser - Met - Glu - His - Phe - Arg - Trp - Gly - Lys - Pro - Val - $NH_2$ | $10^{-6}$–$10^{-4}$ | Phoenixpeptide; 043–01 |
| NEI-MCH (preproMCH [131–165]) | Glu - Ile - Gly - Asp - Glu - Glu - Ser - Ala - Lys - Phe - Pro - Ile - Gly - Arg - Arg - Asp - Phe - Asp - Met - Leu - Arg - Cys - Met - Leu - Gly - Arg - Val - Tyr - Arg - Pro - Cys - Trp - Gln - Val ~ disulfide bridge between Cys152 and Cys162 | $10^{-5}$–$10^{-4}$ | Phoenixpeptide; 070–30 |
| Amidated proline-valine dipeptide (PV-$NH_2$) | Pro-Val - $NH_2$ | $10^{-6}$–$10^{-3}$ | Innovagen AB |
| Amidated proline-isoleucine dipeptide (PI-$NH_2$) | Pro-Ile - $NH_2$ | $10^{-6}$–$10^{-3}$ | Innovagen AB |